

re Paul Greyer  
project reviewed  
at IRB mtg.  
11/25/86

# Nitrogen gas exchange in the human knee

P. K. WEATHERSBY, P. MEYER, E. T. FLYNN,  
L. D. HOMER, and S. SURVANSKI

Hyperbaric Medicine Program Center, Naval Medical Research Institute, Bethesda, Maryland  
20814-5055; and Lawrence Livermore National Laboratory, Livermore, California 94550

WEATHERSBY, P. K., P. MEYER, E. T. FLYNN, L. D. HOMER, AND S. SURVANSKI. *Nitrogen gas exchange in the human knee*. *J. Appl. Physiol.* 61(4): 1534-1545, 1986.—Human decompression sickness is presumed to result from excess inert gas in the body when ambient pressure is reduced. Although the most common symptom is pain in the skeletal joints, no direct study of nitrogen exchange in this region has been undertaken. For this study, nitrogen tagged with radioactive  $^{13}\text{N}$  was prepared in a linear accelerator. Nine human subjects rebreathed this gas from a closed circuit for 30 min, then completed a 40- to 100-min washout period breathing room air. The isotope  $^{13}\text{N}$  was monitored continuously in the subject's knee during the entire period using positron detectors. After correction for isotope decay (half-life = 9.96 min), the concentration in most knees continued to rise for at least 30 min into the washout period. Various causes of this unexpected result are discussed, the most likely of which is an extensive redistribution of gas within avascular knee tissues.

inert gas kinetics; tracer; decompression sickness; nitrogen isotope; positron emission

HUMAN DECOMPRESSION SICKNESS (DCS) is presumed to follow a supersaturation of inert gas and formation of bubbles that occurs when the rate of pressure reduction is too fast compared with the rate of gas elimination. Experimentally derived gas kinetics have not been available. Symptoms of DCS can occur in many organ systems, but the most common presentation is pain in the skeletal joints. The knee is the primary focus of pain in approximately 30% of deep-sea divers presenting symptoms of DCS. Indirect evidence from numerous studies in decompressed aviators supports a local source for this pain (20). This suggests that the knee may be peculiar in its gas exchange.

Nitrogen gas exchange in organs was studied directly by Campbell and Hill (5) in the early part of this century and more recently by Thomas et al. (28). Most studies since then have concerned centrally sampled gas (venous blood or expired air), which cannot be used to infer kinetic behavior of any specific organ (1). Insight into partially localized gas exchange may be achieved using inhaled radioisotopes and external detection. Several animal studies performed with  $^{133}\text{Xe}$  were directed toward the entire animal or the joints in particular. The  $^{133}\text{Xe}$  isotope was also used in many human studies of local blood flow, especially within the brain and skeletal muscle. Our survey in dogs with a large-field gamma detector showed an unusually slow exchange of  $^{133}\text{Xe}$  in

the shoulder joints and knees (31). Others (27) have shown skeletal retention of xenon for several days. When radioactive argon is formed in bone mineral by activation of calcium, the excretion rate is very prolonged (2). Direct injection of xenon into the knee is followed by redistribution of the isotope through several nearby tissues (24) and an overall slow rate of excretion (26). Inert gases exchange slowly in human knees.

Isotopes of the inert gases normally used for diving, nitrogen and helium, are not commonly available. There is no usable isotope of helium and all radioisotopes of nitrogen are short lived. The most promising, positron-emitting  $^{13}\text{N}$ , must be studied at the site of production because it decays at a half-life of 9.96 min. Apparently, this isotope has not been used to study nonpulmonary tissues, but its use in decompression studies was suggested by West (33).

This work was designed to obtain quantitative measures of nitrogen exchange rates in human knees using a radiotagged nitrogen tracer. Data would be used to evaluate physiological models of gas exchange and provide a data base for decompression calculations. The results, however, were unexpected, indicating a rise in knee nitrogen concentration for more than 1 h after a change in inspired gas gradient. The best explanation is a significant flux of gas into a local sink that coincides with the most sensitive area for detection with the specific instrumentation employed.

## METHODS

*Experimental.* Each subject inspired a normoxic gas with radioactive  $^{13}\text{N}_2$  for 30 min and room air for a 1.5-h washout period thereafter. Isotope activity was monitored by two detectors: one of 13 cm diam and the other a 40-cm-diam positron camera. In *experiments 1-7* the small detector was aligned over the left knee and the camera over the upper extremities. In *experiments 8 and 9*, the camera was over the knee and the small detector on an inspiratory section of the rebreathing circuit. Details of isotope production and detection are in APPENDIX 1.

The breathing circuit is shown in Fig. 1. After production, the  $^{13}\text{N}_2$  was analyzed for ozone (< 0.1 ppm) and  $\text{NO}_2$  (< 2 ppm). Then about 50 liters of the  $^{13}\text{N}_2$  were mixed with pure  $\text{O}_2$  to reach a final concentration of  $20.8 \pm 0.2\%$   $\text{O}_2$ . The  $\text{N}_2\text{-O}_2$  mixture was kept in a 100-liter gas bag behind a 1-cm lead shield to minimize personnel exposure and camera overload. The bag was connected

REPOSITORY LLNL T5627 Rm 1000

COLLECTION Navy Diver Documents

BOX No. \_\_\_\_\_

FOLDER Human Subjects TASK Force

TASK No 3 File No. 4

MAC 1994

1106869

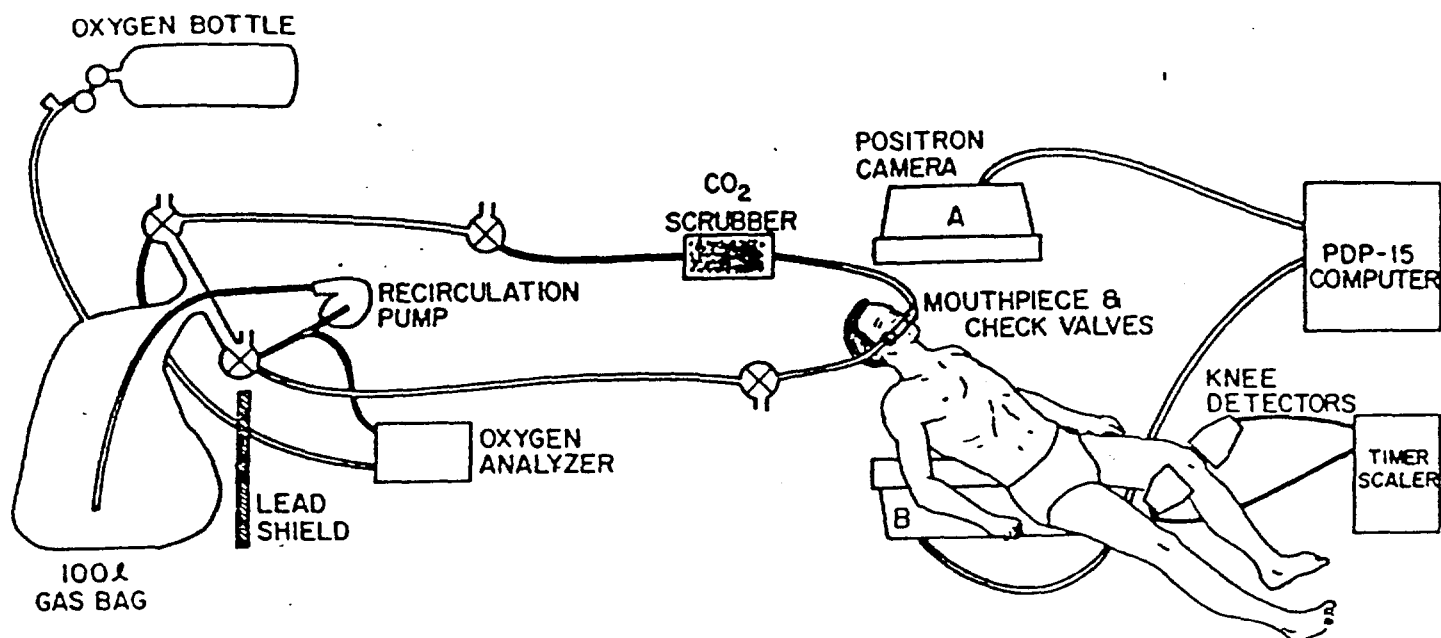


FIG. 1. Experimental apparatus. See text for details.

to a rebreathing circuit consisting of 12 m of 4-cm-ID tubing, low-resistance valves, a CO<sub>2</sub> scrubber, and a mouthpiece. Gas was pumped continuously from top to bottom of the gas bag at 8 l/min to enhance mixing. Supplemental experiments using two inert gases and a mass spectrometer showed that the gas concentration in the rebreathing circuit would reach about 85% of steady state within 1 min of the start of an experiment. Before and during rebreathing, O<sub>2</sub> was monitored with a polarographic electrode (Beckman OM-11). Fresh O<sub>2</sub> was added through a manually adjusted needle valve to maintain the circuit between 0.2 and 0.4% O<sub>2</sub> of the starting value. No breathing resistance was reported by any of the subjects.

Each subject took three rapid, deep breaths at both the start and finish of rebreathing to expedite mixing in the circuit and the lungs. Those breaths were comparable with the volume of tubing in the rebreathing circuit. The study was designed to measure <sup>13</sup>N<sub>2</sub> kinetics during a 30-min uptake phase of constant inspired concentration of <sup>13</sup>N<sub>2</sub> and a washout phase of up to 105 min of breathing room air (Fig. 2). This time interval was considered the maximum possible study time because it covered 13 half-lives of <sup>13</sup>N. After such a time, the count rate was 2<sup>-13</sup> of the original or a reduction by a factor of well over 1,000. Durations of experiments varied 80–135 min before detectors reached essentially background levels of radiation. Counting intervals ranged from 0.5–5 min, depending on the count rate. After the 30-min rebreathing period, the subject breathed room air through a valve near the mouthpiece, and expired gases were vented outside. Subjects remained motionless throughout the study period and were covered with a blanket that kept them comfortably warm.

Nine male volunteers served as subjects after providing informed consent (Table 1). Subjects in experiments 1–6, 8, and 9 were experienced deep-sea divers; only the subject in experiment 7 was a smoker. By the operation

of the LINAC at maximum power and steady state, a specific activity of 1.7 mCi/l of radioactive nitrogen was produced. Before each experiment, radiological decay and dilution in the circuit and the subject's lungs reduced the initial inhaled specific activity to a maximum of 0.2–0.3 mCi/l. The calculated internal radiation dose was 350–450 mrad to the lungs and half of that range to the trachea. Doses for other internal organs from local positron annihilation and from gamma radiation in the lung gas were estimated at under 10 mrad. External dosimeters provided readings consistent with this estimate.

*Data analysis.* The dominant feature of the raw data was the <sup>13</sup>N radiological decay rate as illustrated with a hypothetical example in Fig. 2. The desired inspiratory profile was a square wave of 30 min duration (solid trace at top). By decay alone, emissions from a sealed container of <sup>13</sup>N<sub>2</sub> would be recorded as the decreasing trend of triangles. In the absence of radioisotope decay, tissue <sup>13</sup>N concentrations would be expected to show a gradual rise and fall like the dotted line. Radiological decay would make the detected signal follow the time course indicated by squares. These two curves were produced by multiplying each expected curve by an exponential decay function with a 9.96-min half-life. The rate of biological uptake in the tissue could be equaled and then exceeded by decay even before the end of <sup>13</sup>N inspiration (about 15 min in the example shown), producing an apparent maximum signal early in the experiment.

Decay became progressively important during the latter experimental period. Data collection continued until the count rates were near the background level (~1 cpm). At that point the reduction of activity was more than 1,000 times. Interpretation of data relied critically upon accurate correction for decay and background, especially in the latter phases. The usual treatment was to subtract background from raw count rate, then multiply by a decay correction term:  $\exp [+\ln(2) \times t_m/9.96]$ , where  $t_m$  is the appropriate mean time of the sample period. The

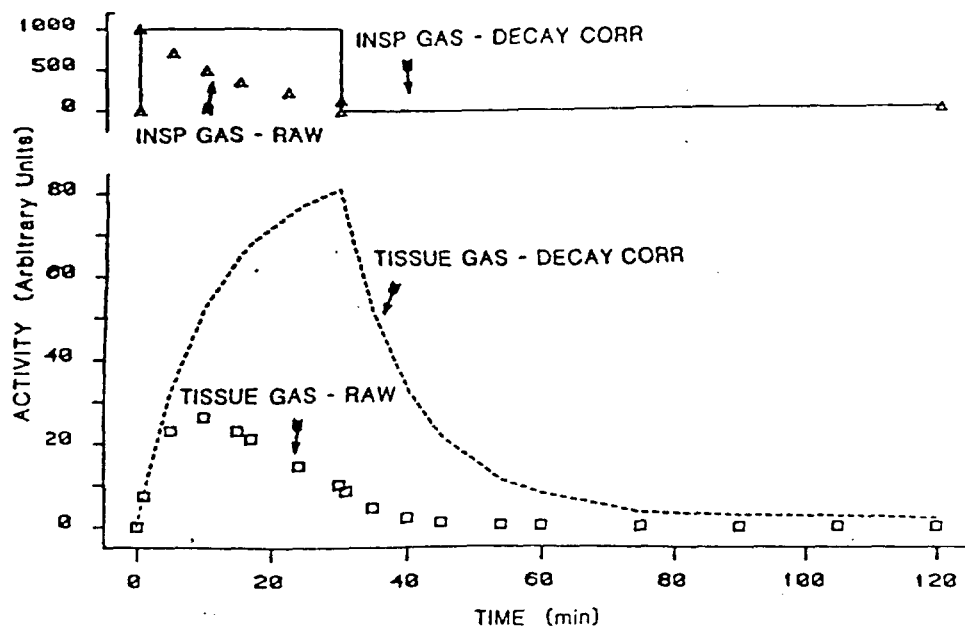


FIG. 2. Hypothetical data expected from experimental design.  $^{13}\text{N}_2$  mix was to be inspired at constant (decay-corrected) concentration for 30 min and recorded over numerous tissues for that period and a washout period. Radiological decay was expected to alter the curves by an exponential decay with a half-life of 9.96 min.

TABLE 1. Subject information

Exp No.	Age, yr	Ht, cm	Wt, kg
1	35	165	65
2	24	155	79
3	28	191	82
4	26	173	71
5	28	180	68
6	39	182	90
7	31	180	84
8	41	183	92
9	35	183	100

decay correction, therefore, increased the measured  $^{13}\text{N}$  activity to the value that would have been recorded if the isotope had not decayed. For short counting times,  $t_m$  was essentially the midpoint of the counting interval, but longer times required a slight correction as shown in APPENDIX 2. Poisson counting errors (SD = square root of the total counts recorded in a given interval) were multiplied by the same decay correction term. To allow smoother plotting of the data in subsequent figures at times of low count rate, successive counts were combined to yield a statistically useful number of total counts (usually 50) in the extended time interval.

## RESULTS

Figure 3 shows the degree of  $\text{O}_2$  and  $^{13}\text{N}$  control achieved during the 30-min rebreathing period of *experiment 8*. The closed circuit maintained an  $\text{O}_2$  concentration of 20.8–21.0% during the entire period (upper trace). Similar  $\text{O}_2$  control was achieved in all other experiments. The square symbols of Fig. 3 plot the raw counts of radiation recorded over a section of inspiratory hose. Some lag is seen in the first (1 min) point, but a smooth exponential fall is apparent thereafter. Decay correction of the hose activity is also plotted in Fig. 3. The decay-corrected  $^{13}\text{N}$  concentration had a coefficient of variation of about 4%. The variation probably reflects slight leakage, uptake of the isotope into body tissues, and slight

dissolving of  $\text{N}_2$  in the water condensed throughout the rebreathing apparatus. The data of *experiment 9* are similar. These inspired  $^{13}\text{N}$  measurements were not performed in *experiments 1–7*, but all experiments followed the same gas mixing and inspiration protocol.

Raw data from the knee detectors in *experiment 2* are plotted in the upper panel of Fig. 4. All other experiments yielded the same general appearance. Counts increased for 10–15 min to a peak and decreased rapidly thereafter. No break in the data curves was apparent at the 30-min point when the gas mixture was changed from the  $^{13}\text{N}$  mixture to room air. The decay correction can be illustrated with data drawn from Fig. 4. Between 104.0 and 106.0 min, 196 counts were recorded from the knee. The raw activity was thus 98.0 cpm reported at a mean time of 105.0 min. (The formula in APPENDIX 2 shows only a slight error was involved when choosing the midpoint.) The approximate ( $\pm$ SD) uncertainty was 14 counts or 7.0 cpm. A 19-min background check performed less than 1 h later with this detector yielded three counts in 19 min for a rate of  $0.16 \pm 0.09$  (SD) cpm. The net  $^{13}\text{N}$  knee activity was thus 97.8 cpm with a combined uncertainty of 7.1 cpm, assuming the independence of the data and background measurements. Decay correction back to the start of the experiment for  $t_m = 105.0$  min was  $\exp[0.693 \times 105.0/9.96] = 1,489$ , so the corrected knee activity reported was  $(1.46 \pm 0.10) \times 10^5$  (SD) cpm at 105.0 min. In this example, deliberately chosen to be extreme, the strong decay correction still allowed a useful precision, even though the measurement was made more than 1 h into the washout period.

Performing the same type of background and decay correction for all the data of *experiment 2* yielded the curve shown in the lower panel of Fig. 4. For this and Fig. 5, two SD error bounds were plotted. The initial rise in activity continued throughout the measurement period, even more than 1 h after the end of  $^{13}\text{N}$  breathing. The uncertainty due to strong decay correction increased continuously until the signal-to-background ratio made

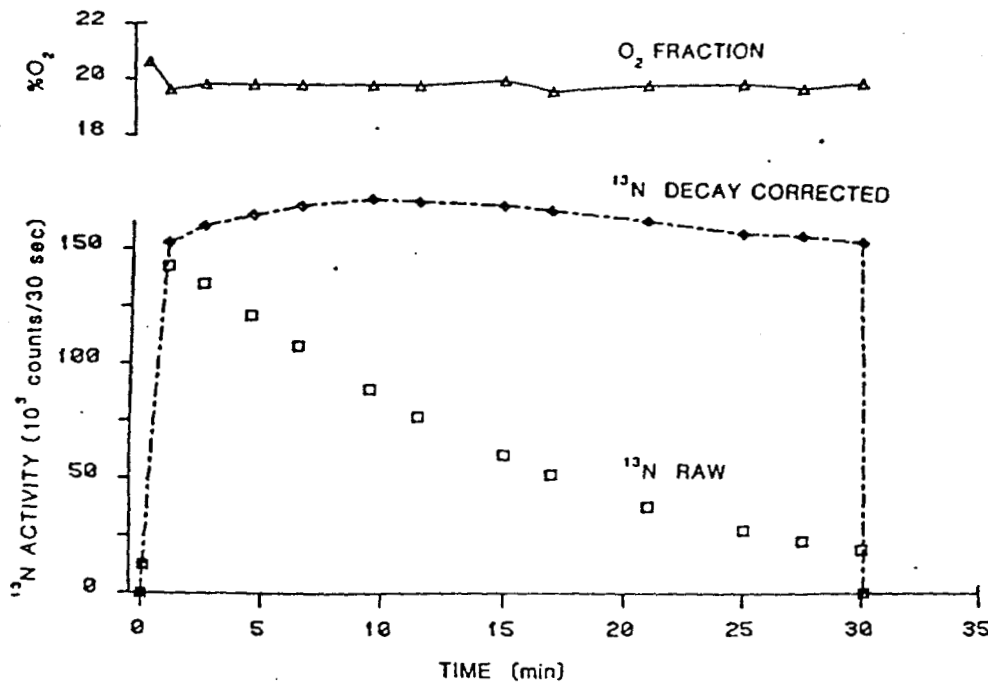


FIG. 3. Inspiratory gas measurements from experiment 8. O<sub>2</sub> (top) and <sup>13</sup>N (bottom) in inspired gas monitored during experiment. Radioactivity measured (squares) was subject to decay correction (diamonds).

the data unusable beyond approximately 115 min. Nevertheless, the relentless rise in corrected <sup>13</sup>N<sub>2</sub> activity during most of the experiment was much greater than experimental counting error.

Decay- and background-corrected data for all other experiments are shown in Fig. 5. The background ranged from 0 to 12 counts in 10 min for experiments 1-7, and a single average background of 0.28 cpm was used. The larger detectors (with less lead shielding) used in experiments 8 and 9 resulted in a background of 4 cpm. Nevertheless, the greater signal-to-background ratio allowed those experiments to continue beyond 2 h. Comparison of absolute count rate among subjects was not warranted because of variations in amount of <sup>13</sup>N<sub>2</sub> produced, differences in detector tuning, subject size, and exact location of the knee in the detector field. With the possible exceptions of experiments 4 and 7, all subjects' knees showed an unmistakable rise in <sup>13</sup>N<sub>2</sub> activity after the subjects stopped breathing <sup>13</sup>N<sub>2</sub>.

The original intent to compare these knee data with exchange in upper body sites recorded by the large positron camera has been frustrated by data analysis problems. An example is shown in Fig. 6. These are decay- and background-corrected activity in the upper arm (mostly muscle) in experiment 4. Regional activity was extracted from the full camera data by the weighted backprojection method of Lim et al. (18) using eight iterations and a power of one. Nineteen time intervals of up to 10 min duration were independently reconstructed, with the midpoint of the time interval used for plotting in Fig. 6. Despite the substantial error bounds, the data behave more "normally" than the knee. Soon after the switch in inspired gas the activity dropped significantly and maintained a low level thereafter.

Figure 6 was chosen as our best example of an anatomic area in these studies with a clearly different kinetic response from the knee. Other reconstructions show generally similar shapes: rise for 30 min, fall rapidly at

30 min, and weakly rise or fall thereafter with a large amount of apparent random changes. The error bars displayed in Fig. 6 are  $\pm$ SD counting error; the reconstruction must introduce some additional but currently unknown error.

#### DISCUSSION

The marked rise in knee <sup>13</sup>N levels relatively long after the end of radioactive gas inspiration was unexpected. We had anticipated the possibility of very slow kinetics that would appear as a nearly linear rise for 30 min followed by a decrease so slight as to appear nearly horizontal. From Figs. 4 and 5 it is apparent that exchange is even slower, resisting the gradient for excretion for at least an hour. It is necessary to examine whether this result was due to a specific technical artifact, then to discuss mechanisms for very slow nitrogen exchange, and finally to postulate how the specific late rise could be observed.

*Technical questions.* Possible technical artifacts were examined in detail at the time of the experiments and during the 20-mo interval between experiments 1-7 and 8 and 9. The correct position of the inspiratory valve on shift to room air was verified several times, and the rebreathing circuit itself was vented to the outside of the building within 10 min of the end of rebreathing. Timers and energy discriminators were examined repeatedly; the energy discrimination circuits showed a small amount of drift as is common but nowhere near enough to change detector response by more than a few percentage points.

The possibility of pulse pileup during the early stages of the experiment would have caused output to saturate during the run. When this occurs, gamma rays frequently arrive at the detector before a previous event has been analyzed for the proper energy; one or both events are then rejected. The large detector resolving time, however, was  $<10 \mu$ s and the small detector resolution time was 1  $\mu$ s. Thus pileup would only be significant at gamma-ray arrival rates of  $10^5$ /s or faster. Calculations using the

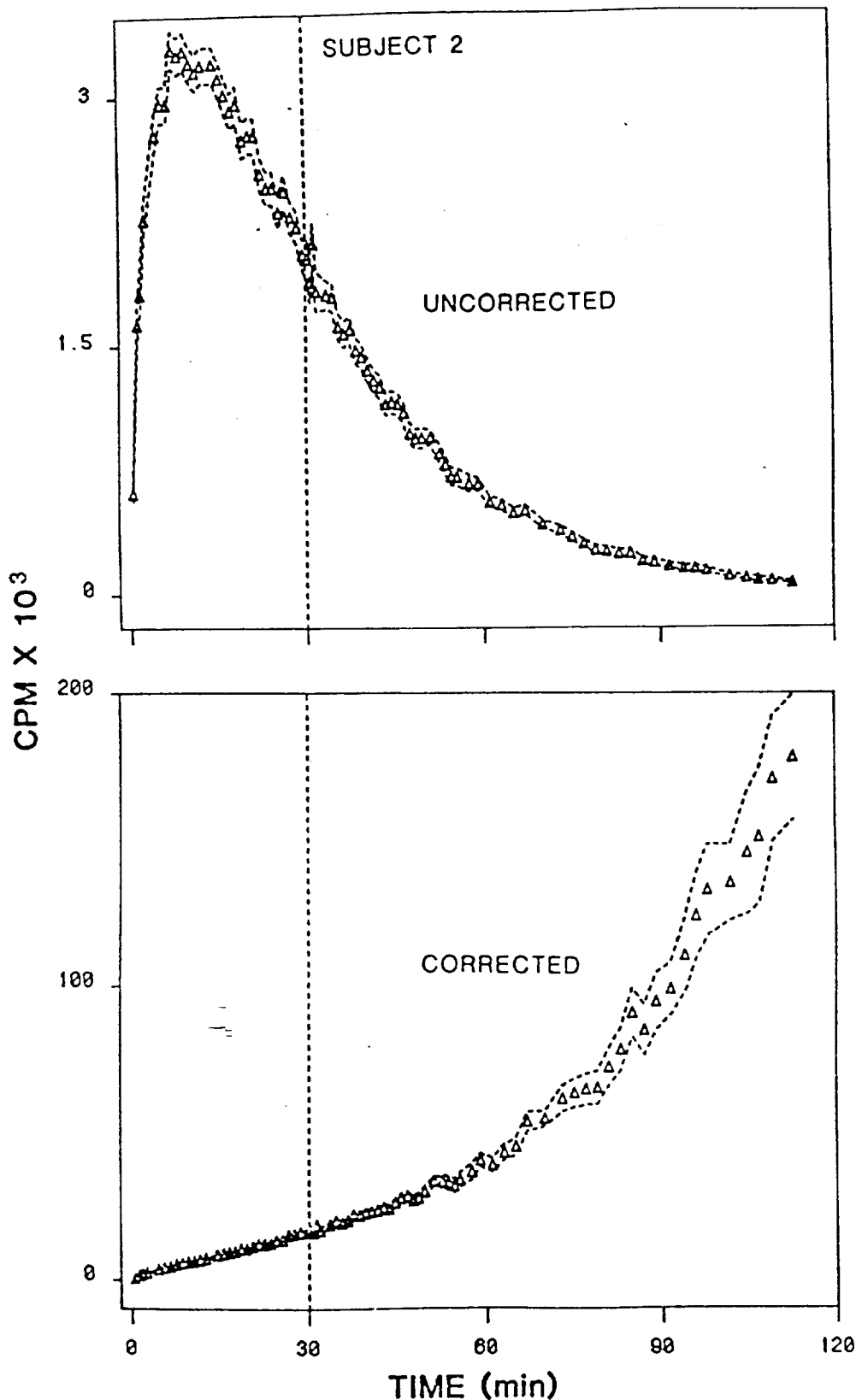


FIG. 4. Top: raw radioactive emissions (in thousands of counts/min) from  $^{13}\text{N}_2$  decay in the knee (*experiment 2*). Each triangle is a raw count rate from a counting interval of 0.5–3 min. Dashed lines are 2 SD bounds on counting (Poisson) error. Bottom: decay-corrected emission rate from same knee after background and decay correction as described in text. Two SD error bounds were treated similarly. Dashed line at 30 min is end of  $^{13}\text{N}_2$  inspiration and beginning of washout.

specific conditions of *experiments 1–7* show that even counting gamma rays that do not arrive in coincidence (about 60 times greater than the coincidence rate) would not put the knee detector in a pileup situation. In other performance checks with the large detector, coincidence rates of 6,500 counts/s were measured accurately without significant pileup. The danger became much smaller later

in the experiment when all  $^{13}\text{N}$  gas sources were vented outside and knee events fell below 10 counts/s but continued the decay-corrected rise. We noted that pileup problems did occur with the large detector in *experiments 1–7* when upper-body exchange rates were sought.

Gamma-ray flux from sources other than the knee could also yield a spuriously high count. These rays have

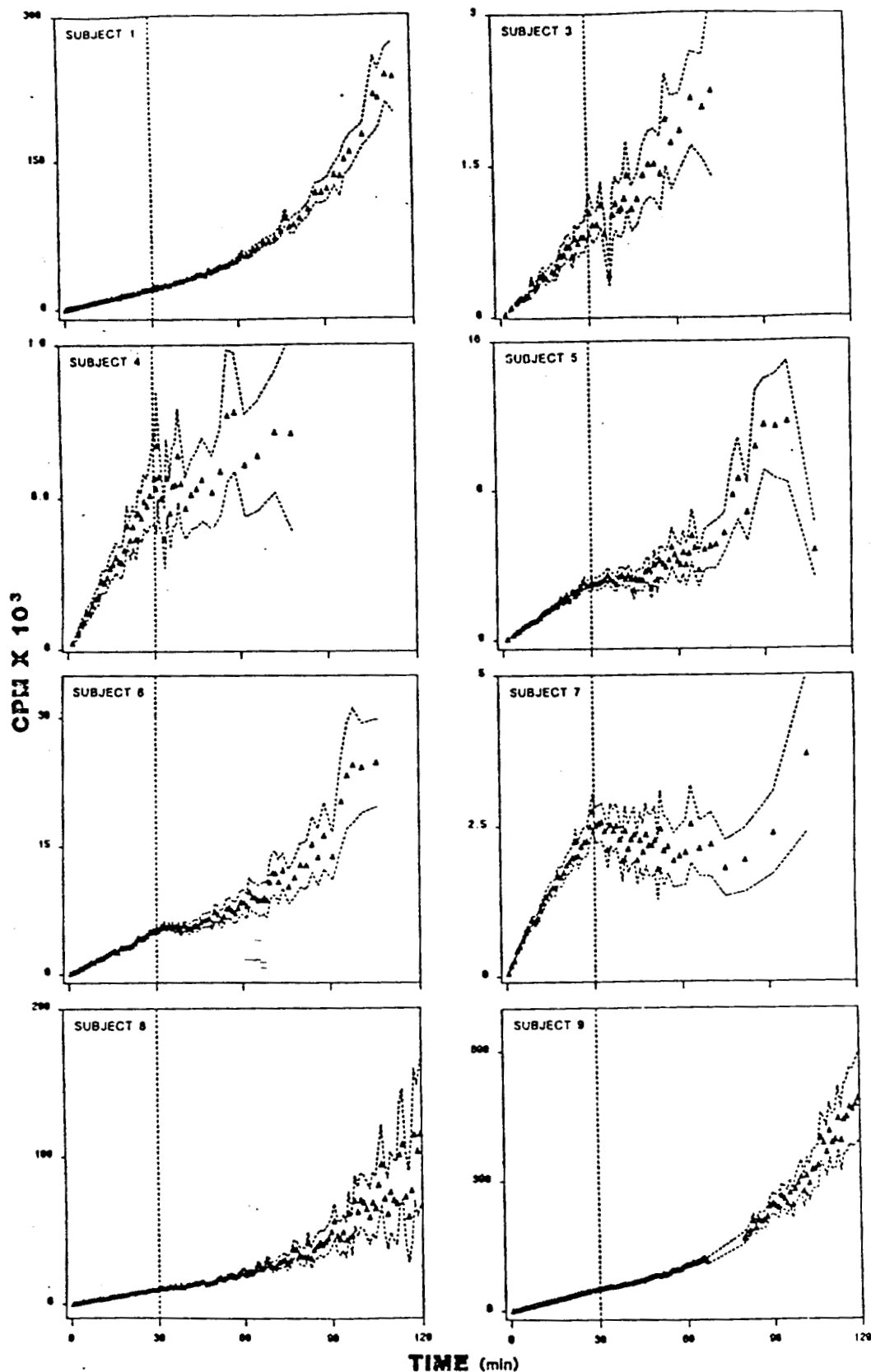


FIG. 5. Decay-corrected emission rates (in thousands of counts/min) from knees in 8 other experiments. Raw data were subject to background and decay correction as described in text. Two SD error bounds were treated similarly. Dashed line at 30 min is end of <sup>13</sup>N<sub>2</sub> inspiration and beginning of washout. One crystal in positron camera was inoperative during period 65–80 min in experiment 9.

to be treated as background for purposes of analysis. Many repeated background measurements before and after the study gave readings far too low to seriously affect the data. Of course background counts cannot be directly determined during the experiment and the nearby nonknee sources of radiation are a concern. In

control experiments in which a 3-liter gas bag of <sup>13</sup>N<sub>2</sub> in the approximate position of the subject's lungs was used; however, detectors with 5 cm of lead shield, located where the knee would have been, registered many orders of magnitude lower activity than that of the bag. Extra lead shielding around the detectors kept this effect under

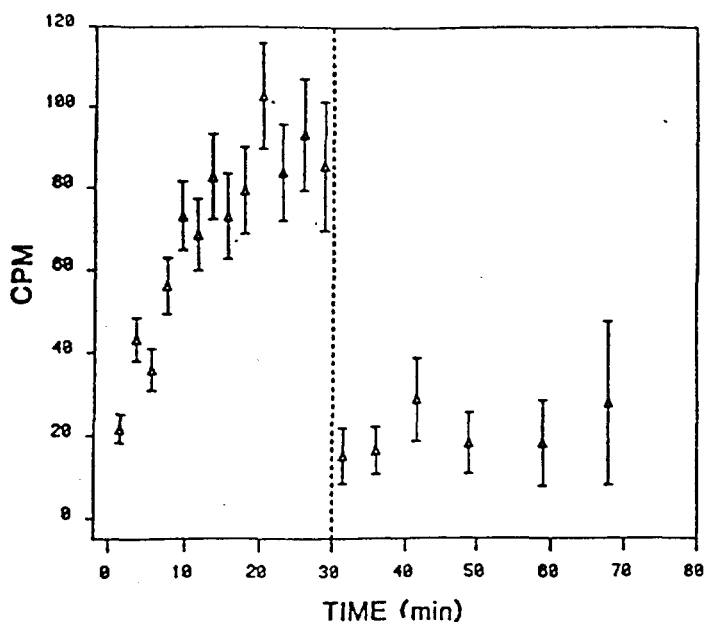


FIG. 6. Decay and background corrected emission rate from upper arm in *experiment 4*. One SD error bound were corrected similarly. For this region, background activity was well below 1 cpm.

control. This artifact was thus avoided, but even if it had been present, it would have become unimportant in the latter phases of the experiment when the only significant activity in the room was in the subject's body.

The very large decay correction required makes the decay rate of the gas an important question. The treatment of isotope decay presumes all the isotope is  $^{13}\text{N}$ . Should contaminant gases be present, the data could be affected severely. The nitrogen for this experiment was purchased as a very pure gas. With the same accelerator and gas-handling equipment, gases containing positron emitting isotopes  $^{15}\text{O}$  and  $^{11}\text{C}$  were irradiated on other occasions. These were made with the same ( $\gamma, n$ ) nuclear reaction but with  $\text{CO}_2$  or  $\text{O}_2$  in the LINAC beam. None of these radioactive gases can be differentiated on the basis of their emitted gamma rays because all decay by positron annihilation and produce pairs of 511 KeV gamma rays identical to those from  $^{13}\text{N}$  decay.

The decay rate of gas used in this study was addressed in several additional experiments where  $^{13}\text{N}$  was produced in an identical manner but not exposed to humans. The gas was kept in a steel cannister or in a 20-liter gas bag. Activity/time records were made of the isotopic decay, such as those in Fig. 7. The semilog plot in this case is quite straight over four orders of magnitude, indeed up to the point where detector background was reached. The slope of this plot is equivalent to an isotope half-life that agrees with accepted values within 1-2%. The uncertainty in the half-life is such that a 1% error in half-life propagates a 7% uncertainty in corrected activity at  $t_m = 105$  min. As shown in Fig. 7, the standard background and decay treatment returned the  $^{13}\text{N}_2$  plot to a constant over several hours (square symbols). Attempts to analyze the data of Fig. 7 to extract a second half-life (i.e., an isotope contaminant) yielded upper bounds of about 0.01% for the most likely contaminant ( $^{11}\text{C}$ , half-life = 20 min) and lower ones for other candidate isotopes.

Additional estimates were made of possible contaminant levels. In one test,  $^{13}\text{N}$  produced in the standard way was bubbled through a caustic bath [mixed  $\text{Ca}(\text{OH})_2$  and  $\text{NaOH}$ ] to trap any acid gases that might have been produced (e.g.,  $\text{NO}_2$ ,  $\text{NO}_3$ ,  $\text{HCN}$ , or  $\text{CO}_2$ ). In this experiment, the acid-free gas showed a normal  $^{13}\text{N}$  decay. The residual liquid was counted as well, but the data were complicated by a diffusion exchange between air and gas spaces. When a diffusion model was used to account for this effect, the decay appeared once again to consist completely of  $^{13}\text{N}$  with an upper bound of 0.2%  $^{11}\text{C}$  of the possible original abundance of  $^{13}\text{N}$ . Because gas diffusion altered the counting geometry, this experiment had a larger uncertainty than the analysis of Fig. 7.

Finally, estimates were made of the gas mixture used in *experiments 8* and *9*. After the end of the inspiration phase, part of the rebreathing circuit was isolated by valves and the inspired gas detectors continued to run. The data during the next several hours were noisier than Fig. 7, but analysis of the decay showed about 1% of an  $^{11}\text{C}$  component in the  $^{13}\text{N}$ .

What would be the effect of isotopically contaminated gas? Even substantial amounts of  $^{15}\text{O}$  gas would not become a problem because it decays at a half-life of 2 min. Furthermore, none of the gas prepared for these experiments had even a chemically measurable trace of ozone or nitrogen oxides, which are usually detected when a source gas containing  $\text{O}_2$  is irradiated. If, however, a substantial fraction of the original gas was a slower decaying isotope than  $^{13}\text{N}$ , our decay correction would produce an inappropriate increasing curve. The  $^{11}\text{C}$  could be a problem because it decays at half the rate of  $^{13}\text{N}$  (half-life = 20.4 min). The possibility of  $^{11}\text{C}$  contamination leading to these results can be examined as follows. Assume that the  $^{11}\text{C}$  is delivered in an isotopic form such as  $^{11}\text{CH}_4$ , which has the same physiological exchange rate properties as nitrogen (22, 23). As both isotopes distribute throughout the body, the  $^{13}\text{N}$  tracer will decay faster and let a relatively higher fraction of subsequent emissions come from the  $^{11}\text{C}$  tag. Each isotope fraction would have to be decay corrected individually to avoid a misleading rise in decay-corrected data.

Decay-corrected curves assuming various fractions of  $^{11}\text{C}$  in the knee are presented in Fig. 8 using the raw data of *experiment 2* as before. Any fraction up to about 1%  $^{11}\text{C}$  in  $^{13}\text{N}$  scarcely changes the corrected curves. Higher levels bring the later phase of the curve down to lower levels. For this experiment, even 10%  $^{11}\text{C}$  did not force the corrected curve to decrease at the start of washout. Similar calculations show that an original fraction of 5-30% (1% in *experiment 7*) of the original positron-emitting isotope would have to be  $^{11}\text{C}$  for the decay-corrected curves to appear flat after 30 min. Evidence against this high a contaminant level are the facts that the gas was originally purchased as a mixture with less than 1 ppm hydrocarbon, and the activation cylinder and transfer lines were kept in a vacuum when not in use for  $^{13}\text{N}$  activation (<1 mTorr). As shown above, half-life analysis could support 1% at most of original  $^{11}\text{C}$  fractional activity. Other isotopic contaminants are even less likely because they would have to emanate from the experi-

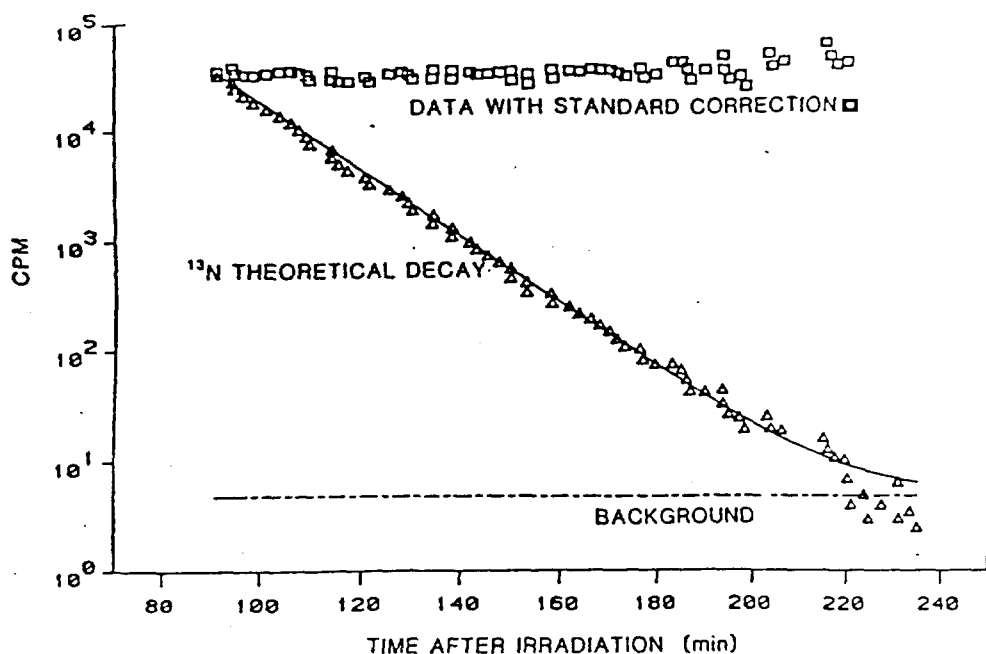


FIG. 7. Radiological decay of  $^{13}\text{N}_2$  sample. Gas was prepared as described in text and kept in a 30-liter gas bag in positron camera for 4 h after irradiation. For first 70 min after preparation radiation was too intense for true recording (see discussion of pileup in text). Thereafter, 30-s to 10-min counts (triangles) were made until gas decayed to essentially background levels. Solid line is a best-fit least-squares regression to data of a single exponential decay (time constant 9.96 min) with an estimated constant background.

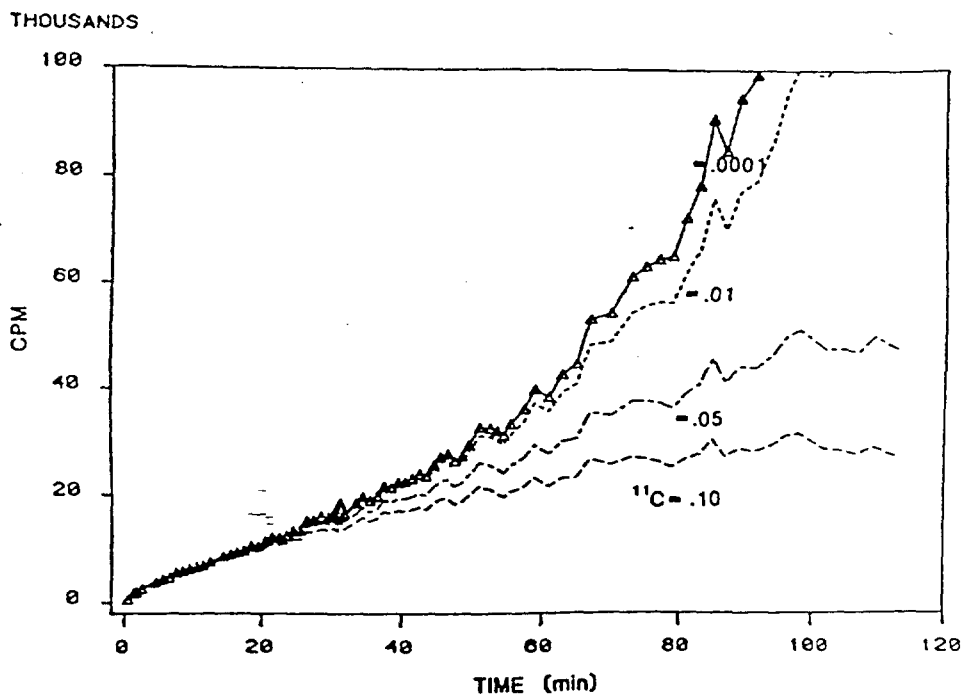


FIG. 8. Effect of  $^{11}\text{C}$  contamination in isotope decay correction. Data of experiment 2 (Fig. 4) were corrected for decay and various assumptions were made about fraction  $^{11}\text{C}$  with dominant  $^{13}\text{N}$  isotope present in the knee: no contamination (triangles); 0.0001  $^{11}\text{C}$  (solid line); 0.01  $^{11}\text{C}$  (dotted line); 0.05  $^{11}\text{C}$  (dashed-dotted line); and 0.10  $^{11}\text{C}$  (dashed line).

mental materials, be delivered as gases with high specific activity, and emit positrons. Finally, one other sample of gas prepared in this system was sent to another laboratory for a complete nuclear spectrum analysis. Only  $^{13}\text{N}$  (no other isotope) was reported.

The most extreme form of a contamination hypothesis we can imagine is a contaminant of  $^{11}\text{C}$  in its maximum plausible concentration, about  $10^{-3}$  of  $^{13}\text{N}$ . The  $^{11}\text{C}$  would need to be tied chemically to a molecule whose synthesis could proceed in the extremely active environment of high radiation field bombardment, and the chemical form of the  $^{11}\text{C}$  would have to be subject to extreme biological amplification (i.e., HCN). The initial entry rate of the HCN into the subjects would be proportional to its abundance, and nearly all of it reaching the alveoli would

be picked up in the blood and delivered to tissue. Because cyanide is essentially irreversibly bound to oxidative enzymes in tissue, its rate of biological excretion would approach zero. Thus almost every molecule of HCN would be delivered to the body and conceivably remain at its peak level in any tissue for the duration of the experiment. Local knee activity, however, would have to approach the fraction of  $^{13}\text{N}$  already stated as needed to render the curves of Figs. 4 and 5 flat after 30 min (5-30% of the  $^{13}\text{N}$  local activity). This is also unlikely quantitatively, and no mechanism is known to make the knee especially susceptible to cyanide poisoning. Our additional but problematic data from other tissues in the same experiments do not show the large rise in concentration of  $^{13}\text{N}$  after switching to room air as the breathing

mixture.

One problem with data from other regions such as shown in Fig. 6 is the very low level of activity and consequently large error bounds. The low level is a result of choosing a small region far from the lungs, mouth, and nose. The shape of the curve during the hour following gas switching cannot be accurately established; slight rise and slight fall are both consistent. The most important use of these data in the present context is to conclude that some areas in our subjects did not have a continual upward trend in tissue  $^{13}\text{N}_2$  concentration. The fall in corrected activity after 30 min appears convincing, but more problems are possible. Suppose that the data for the arm arise partially from gas spaces in the breathing circuit or the subject's lungs, parts of which were also in the camera field of view. Then the fall after 30 min could be misleading. Thus the question becomes: how reliable is the spatial reconstruction procedure?

A number of different methods have been published for three-dimensional reconstruction of positron images. However, they are all tested and used in a clinical static setting where isotope doses are much higher and  $10^6$ – $10^8$  counts are accumulated for a single image. (In these experiments  $10^4$  counts were the maximum available after about 40 min.) For Fig. 6 we used an algorithm that avoids susceptibility of common transform methods to low-activity artifacts (18). No reports are available to provide quantitative guidance in its use. We performed some simulations that made the algorithms of Lim et al. (18) and Shepp and Vardi (25) appear promising, but much more work is required before reconstructed images are reliable for quantitative kinetics.

An actual rise in knee  $^{13}\text{N}_2$  activity has been observed. On a finer level, the results in Figs. 4 and 5 do not allow a precise conclusion on how much the nitrogen rose (or fell) in what part of the knee. The detector only reported a single activity averaged over the entire field of view. The rise could mean nitrogen moved in from entirely outside the detector field, or from an area of low detection efficiency to an area of higher efficiency. We can reject the possibility of no gas movement at all, since that would produce a constant  $^{13}\text{N}_2$  activity (after decay correction). All radiation detectors have a field of view with differing spatial sensitivity. Our type of positron detector has a relatively mild variation in sensitivity (3), and we take its behavior into account in the proposed explanation discussed later with Figs. 9 and 10.

*Mechanisms of nitrogen exchange.* It is necessary to consider mechanisms for the observed rise of knee  $^{13}\text{N}_2$ . First, nitrogen would need a long residence time in some knee or nearby structure such that excretion of labeled gas would be very slow during periods of 1–2 h. Such nitrogen sinks could be physical, chemical, or physiological. One physical possibility is a gas bubble phase that would preferentially retain the gas, since nitrogen is about 70 times more soluble in air than in tissues like blood (30). Some theories hold that humans always have a store of gas micronuclei that are available for subsequent enlargement to cause decompression sickness (35). Gas areas can form in the body and persist for some time without any major symptoms. This was demonstrated

clinically in humans after altitude decompression (29) and by routine X-ray or CAT examination (9). Indeed, most of our subjects were divers with a history of decompression conceivably resulting in some persistent bubbles. None of our subjects, however, had undergone decompression for weeks to months, and knee X-rays of subjects 8 and 9 several weeks after the experiments showed no visible gas bubbles. In addition, subjects' legs were normally extended and fully supported so knee-joint traction was not as severe as that used to elicit gas pockets described in radiological examinations (9). Finally, this mode of physical trapping would be possible with any gas species, but the numerous studies using  $^{133}\text{Xe}$  did not report a similar result.

Another form of physical trapping would occur if any gas actually penetrated into bone matrix. Inert gases in those areas can take days to emerge (2). Such a mechanism would have also loaded other bony areas and our unreported data from other joints do not support such a conclusion.

Chemical trapping can occur by any mechanism that transfers the labeled  $^{13}\text{N}$  atom to species other than nitrogen. Many lower organisms have enzymatic systems to fix atmospheric  $\text{N}_2$  into other forms, but reaction of nitrogen is exceedingly difficult without either those enzymes or metallic catalysts at high temperature (16). For several years a series of studies purported to show active nitrogen metabolism in humans (6), but the result now seems to be explained by experimental artifact (11). We consider all chemical mechanisms unlikely, because it is difficult to find a plausible reaction, and the effect seems to occur specifically in the knee.

Physiological transport of inert gas in the knee is complicated by the complex anatomy of the area. Original gas delivery to the area must be from the arterial circulation: bones, articular cartilage, and the synovium have defined vascular systems (10, 14, 17, 34) and could serve as the arterial source of gas. The flows in these tissues are slow, in the range of  $0.01$ – $0.1 \text{ ml} \cdot \text{g}^{-1} \cdot \text{min}^{-1}$ , producing mean residence times as long as 100 min. The circulation is likely to be slower if the joint is immobile (13). Areas in fairly close proximity may have flows differing by a factor of 10 (10). Other areas such as the synovial fluid in the joint space have no blood supply at all and only occasional fluid connections to vascularized bone areas (12, 21). Thus the picture of nitrogen distribution 30 min after the start of inspiration would show some areas approaching their eventual steady-state concentration, others only slightly filled and some areas still nearly devoid of the tracer.

With the rapid drop in arterial concentration, response in many knee structures would not be immediate. Areas perfused more quickly would respond with an immediate and marked drop; areas perfused more slowly would drop but slowly; and areas fed by diffusion would change even more slowly. In fact, diffusion bound areas might well increase in tracer concentration over a period of time because their boundaries would still have a higher concentration than their interiors. In an area with as low a blood supply and blood flow as the knee, the active diffusive redistribution process could be as important as

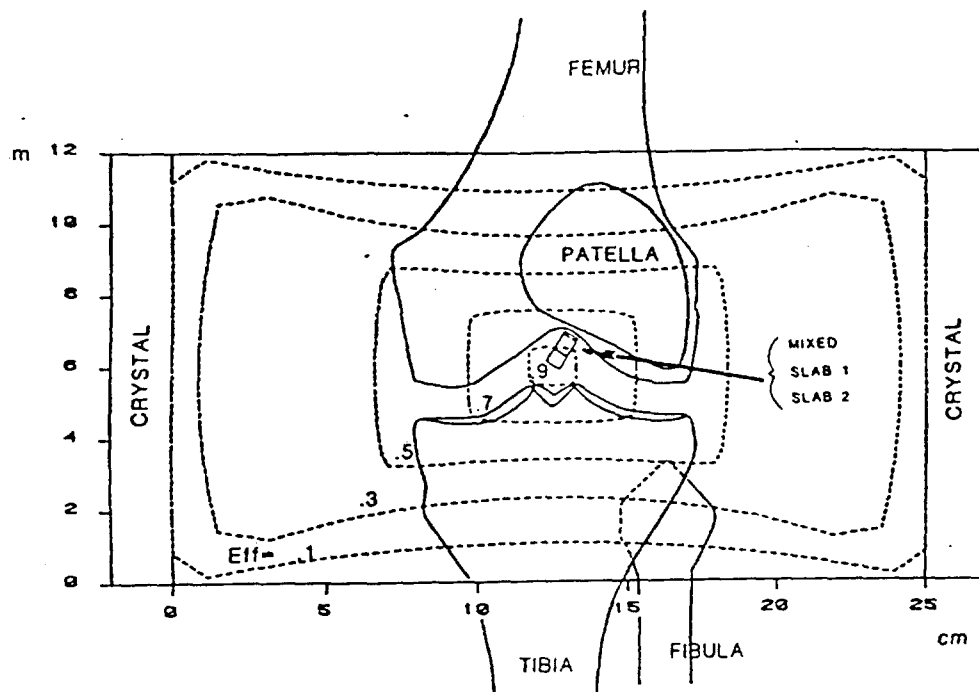


FIG. 9. Detection geometry in the knee during experiments 1-7. Two crystals were aligned with knee-joint line; major bones were approximately in positions as sketched. Dashed lines show relative detection efficiency isosensitivity contours (surfaces of 10, 30, 50, 70, and 90% are shown; maximum detection efficiency was set at 100%). Position of hypothetical mixed and slab compartments referred to in text are also sketched in joint space.

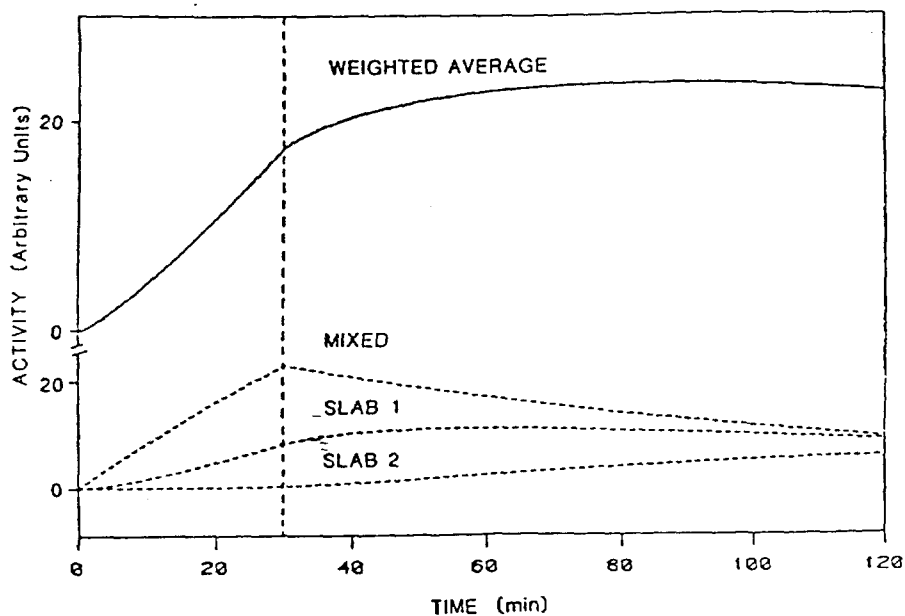


FIG. 10. Simulated data from system of 2 slabs (each 0.5 cm thick) bounded by a well-mixed region 0.1 cm thick on 1 edge as sketched in Fig. 9. Arterial blood was delivered to well-mixed region that had a time constant of 100 min where it passively diffused into slabs with a diffusion coefficient of  $3.5 \times 10^{-5}$  cm<sup>2</sup>/s. Arterial concentration was constant for 30 min and became 0 thereafter. Rise in tracer in all 3 regions is far short of equilibrium, which would be 100 units on scale shown. A hypothetical detector sensed total tissue concentration with relative detection efficiency of 80% (well-mixed region), 90% (first slab), and 95% (second slab). Detector output would appear as traced in upper curve.

venous drainage during the washout phase. One possible transport route follows. The red marrow of long bones has a relatively low blood flow and high partition coefficient for nitrogen (5, 28). In a "short" 30-min exposure this area would be greatly undersaturated in <sup>13</sup>N<sub>2</sub>. During the subsequent 1-2 h it could maintain effluent fluid streams at nearly a constant level of the tracer. It has been reported that direct but presumably very low flow channels connect bone cavity and articular cartilage (12). These channels could serve as sources for prolonged diffusion of gas toward the joint center. The marked redistribution in time after a single intra-articular injection of <sup>133</sup>Xe (24) strongly implies the existence of such diffusive pathways.

*A quantitative possibility.* Formal tracer models of flow plus diffusion transport near the knee are unavailable. Ideally, one would choose a model that realistically in-

cludes prominent anatomic and physiological features of the knee. In addition, one would superimpose the non-uniformity of the particular radiation detector used. Figure 9 is a plot of several isoresponse contours for the detector used in experiments 1-7 calculated from a physical description of detection efficiency (32). The approximate boundaries of the major bones in the knee joint are also sketched. At the center of the detector, roughly at the midline of the joint, the relative efficiency is set at 100%. Efficiency drops below 90% outside a 1-cm region and to 70% within 2-3 cm. The nonvascular synovial fluid and poorly perfused articular cartilage are more efficiently detected than the richly perfused skeletal muscles or bone marrow. This suggests that easily detected regions may acquire tracer largely by pure diffusion from a sluggishly perfused region.

Can diffusion produce the type of kinetics that were

observed? One area of the knee may be modeled very roughly by a pair of adjacent slabs of diffusion-limited tissue 5 mm thick fed at the edge of one slab by a well-mixed region 1 mm thick and with a time constant of 100 min. The diffusion coefficient for nitrogen in this region should be approximately  $3.5 \times 10^{-5}$  cm<sup>2</sup>/s (15), since synovial chemicals do not decrease greatly the diffusion of nitrogen from its value in water (19). The relative counting efficiencies of the mixed area and the two diffusion slabs could be about 80, 90, and 95% of the maximum, respectively. As sketched in Fig. 9, these dimensions and efficiencies can be found in a layer of articular cartilage (mixed area) and adjacent synovial space (slab areas). Finite difference calculations (7) of uptake and excretion of tracer to each region under constant arterial delivery for 30 min are plotted in Fig. 10. The loading of the perfused (mixed) area changes to a drop as soon as the arterial supply ceases; the more slowly loading slabs do not achieve maximum concentration until well after 30 min. The total response weighted for efficiency is the top trace in Fig. 10. It is seen to peak much later than 30 min and has many of the characteristics of the experimental data of Figs. 4 and 5.

Composite curves with the same general characteristics can also be generated using sequences of two or more well mixed tissues if second and latter tissues receive tracer from other mixed compartments rather than arterial blood. Late-rising curves could also be generated even from a well mixed or diffusion limited tissue with a uniform detection efficiency if the gas source was located outside the detector field of view. Experiments with greater spatial sensitivity are needed to decide which possibility is correct.

The unexpected result of a very marked delay in knee gas excretion following pulmonary washout makes further study desirable. No current approach to avoiding decompression sickness uses a gas-exchange model that is consistent with these data; one is now needed.

## APPENDIX 1

### Isotope Production and Detection

The radioactive nitrogen gas <sup>13</sup>N<sub>2</sub> was freshly produced for each subject with a linear accelerator (LINAC) that produced about 500 μA of electrons with a maximum energy of about 72 MeV. Bremsstrahlung photons from the electron bombardment of a heavy metal target induced the <sup>14</sup>N(γ, n)<sup>13</sup>N reaction in a bottle of pure nitrogen (>99.999% N<sub>2</sub>) (Air Products Ultra-Pure Carrier). The decay of <sup>13</sup>N occurs with a half-life of 9.96 min and emits a positron with a maximum energy of 1.2 MeV and a most probable energy of about 0.5 MeV. This particle interacts with an electron near the site of decay, with a range of about 2 mm in water. The interaction results in the annihilation of a positron-electron pair producing two gamma rays of 511 keV energy emitted in exactly opposite directions (8). Detection is possible by external recording of coincident gamma emissions.

The detectors were pairs of NaI(Tl) crystals operated in coincidence: a detection of a 511-keV photon in one crystal was ignored unless a similar photon was simultaneously detected in the other crystal (within about 50 ns). The coincidence feature rejected nearly all radiation unless a positron annihilation event occurred within the cylinder bounded by the two crystal

faces. Thus background radiation was reduced to below one event per second, even without using lead collimation necessary with single-photon isotopes. Due to the limited detector size, the geometric efficiency of detection was reduced to below 25% of the positron events within the field of the crystal. (Because no direction of gamma emission is preferred, events were not detected unless the emission was near the axis connecting the centers of the crystals.)

Two sets of detectors were used. The smaller detector was a pair of crystals 13 cm diam, 5 cm thick, and connected to electronic modules for simple counting of detected coincident 511 ± 30-KeV photons (events) over intervals varying from 30 s to 5 min, depending on the count rate. In experiments 1-7 these crystals were shielded, collimated, and aligned laterally with the joint line of the left knee with a separation of 25 cm. In the final two experiments, this detector pair had a spacing of 15 cm between crystals and was placed around the inspiratory hose.

The larger detector (positron camera) was a pair of scintillation crystals 40 cm in diameter, 1.27 cm thick, and with a crystal separation of 46 cm in experiments 1-7 and 29 cm in experiments 8 and 9. The 37-photomultiplier tube array behind each crystal was connected such that the photon event could be localized within a few mm on the crystal face (3). Each detected event (both cameras "seeing" a photon in coincidence) provided a data point consisting of the x,y coordinates of the photon on each crystal and the time. The data thus included information sufficient to identify a line on which the positron was annihilated. In experiments 1-7 this detector pair was placed over and under the subject's left upper lung lobe, left shoulder, and left lower aspect of the head. In experiments 8 and 9 the camera was placed over and under the left knee. Image recovery of the spatially resolved <sup>13</sup>N<sub>2</sub> concentration is an extremely complicated process (4, 18). Due to the low count rates in this study, reasonable pictures and kinetics could not both be obtained from the data. For reasons discussed in the text, mainly kinetics of the full detector field are reported.

## APPENDIX 2

### Counting Interval for a Decaying Isotope

Suppose that a constant radioactive source is observed over a time interval from  $t_0$  to  $t_0 + \Delta$  while decaying with a time constant [ $\tau = t_{1/2}/\ln(2)$ ] from an initial activity  $A_0$ . We wish to specify the mean time in that interval,  $t_m$ , that is appropriate for the assignment of all measured activity to that time. The total measured counts,  $C$ , over the interval is obtained by the integral of decaying activity over the interval

$$C = A_0 \int_{t_0}^{t_0 + \Delta} \exp(-t/\tau) dt \quad (1)$$

$$= A_0 \tau [\exp(-t_0/\tau)] [1 - \exp(-\Delta/\tau)]$$

This is the same measured quantity that we wish to assign to the source at a single time  $t_m$

$$C = A_0 \cdot \Delta [\exp(-t_m/\tau)] \quad (2)$$

The combination of Eqs. 1 and 2 on rearrangement yields

$$t_m = t_0 - \tau \cdot \ln\{(\tau/\Delta)[1 - \exp(\Delta/\tau)]\} \quad (3)$$

If the sampling interval  $\Delta$  is less than  $\tau/2$ ,  $t_m$  is nearly the midpoint of the interval; for longer intervals  $t_m$  is shifted to earlier times, thus decreasing the magnitude of the decay correction. For example, a counting interval of 10 min with <sup>13</sup>N ( $\tau = 14.4$  min) has  $t_m$  4.72 min after the start rather than 5.00 min, which is the midpoint.

We are indebted to the subjects who volunteered for this study, to K. Byrne and L. Thomas for excellent work on the illustrations, and to D. Temple for editorial assistance.

This research was supported by the Naval Medical Research and Development Command, Research Work Unit No. M0099PN.01-A.0001. The opinions and assertions contained herein are the private ones of the authors and are not to be construed as official or as reflecting the views of the Navy Department or the Naval Service at large.

Received 15 October 1985; accepted in final form 16 May 1986.

## REFERENCES

1. BEHNKE, A. R., AND T. L. WILLMON. Gaseous nitrogen and helium elimination from the body during rest and exercise. *Am. J. Physiol.* 131: 619-626, 1941.
2. BIGLER, R. E., AND J. S. LAUGHLIN. Quantitative analysis of the fate in man of  $^{37}\text{Ar}$  produced in body calcium by fast neutron exposure. *Radiat. Res.* 67: 266-276, 1976.
3. BROWNELL, G. L., J. A. CORREIA, AND R. G. ZAMENHOF. Positron instrumentation. *Recent Adv. Nucl. Med.* 5: 1-49, 1978.
4. BUDINGER, T. F., G. T. GULLBERG, AND R. H. HUESMAN. Emission computed tomography. In: *Image Reconstruction From Projections*, edited by G. T. Herman. Berlin: Springer-Verlag, 1979, p. 147-246.
5. CAMPBELL, J. A., AND L. HILL. Studies in saturation of the tissues with gaseous nitrogen. III. Rate of saturation of goat's brain, liver, and bone marrow in vivo with excess nitrogen during exposure to +3, +4, and +5 atmospheres pressure. *Q. J. Exp. Physiol.* 23: 219-227, 1933.
6. COSTA, G., L. ULLRICH, F. KANTOR, AND J. F. HOLLAND. Production of elemental nitrogen by certain mammals including man. *Nature Lond.* 218: 546-551, 1968.
7. CRANK, J. *The Mathematics of Diffusion* (2nd ed.). Oxford, UK: Clarendon, 1975, p. 141-144.
8. DEBENEDETTI, S., C. E. COWAN, W. R. KONNEKER, AND H. PRIMAKOFF. On the angular distribution of two-photon annihilation radiation. *Phys. Rev.* 77: 205-212, 1950.
9. FUIKS, D. M., AND C. E. GRAYSON. Vacuum pneumoarthrography and the spontaneous occurrence of gas in the joint spaces. *J. Bone Jt. Surg.* 32A:933-938, 1950.
10. GROSS, P. M., D. D. HEISTAD, AND M. L. MARCUS. Neurohumoral regulation of blood flow to bones and marrow. *Am. J. Physiol.* 237 (Heart Circ. Physiol. 6): H440-H448, 1980.
11. HERRON, J. M., H. A. SALTZMAN, B. A. HILLS, AND J. A. KYLSTRA. Differences between inspired and expired minute volumes of nitrogen in man. *J. Appl. Physiol.* 35: 546-551, 1973.
12. HOLMDAHL, D. E., AND B. E. INGLEMARCK. The contact between the articular cartilage and the medullary cavities of the bone. *Acta Orthop. Scand.* 20: 156-165, 1950.
13. INGLEMARCK, B. E. The nutritive supply and nutritional value of synovial fluid. *Acta Orthop. Scand.* 20: 145-155, 1950.
14. KNIGHT, A. D., AND J. R. LEVICK. The density and distribution of capillaries around a synovial joint. *Q. J. Exp. Physiol.* 68: 629-644, 1983.
15. KRIEGER, I. M., G. W. MULHOLLAND, AND C. S. DICKEY. Diffusion coefficients for gases in liquids from the rates of solution of small gas bubbles. *J. Phys. Chem.* 71: 1123-1129, 1967.
16. LEIGH, G. J. Abiological fixation of molecular nitrogen. In: *The Chemistry and Biochemistry of Nitrogen Fixation*, edited by J. R. Postgate. New York: Plenum, 1971, p. 19-55.
17. LEVICK, J. R. Blood flow and mass transfer in synovial joints. In: *Handbook of Physiology. The Cardiovascular System*. Bethesda, MD: Am. Physiol. Soc., 1984, p. 917-947.
18. LIM, C. B., A. CHENG, D. P. BOYD, AND R. S. HATTNER. A 3-D iterative reconstruction method for stationary planar positron cameras. *IEEE Trans. Nucl. Sci.* NS25: 196-201, 1978.
19. MCCABE, M., AND T. C. LAURENT. Diffusion of oxygen, nitrogen, and water in hyaluronate solutions. *Biochim. Biophys. Acta* 399: 131-138, 1975.
20. NIMS, L. F. Environmental factors affecting decompression sickness. Part I. A physical theory of decompression sickness. In: *Decompression Sickness*, edited by J. F. Fulton. Philadelphia, PA: Saunders, 1951, p. 192-222.
21. OGATA, K., L. A. WHITESIDE, AND P. A. LESKER. Subchondral route for nutrition to articular cartilage in the rabbit. Measurement of diffusion with hydrogen gas in-vivo. *J. Bone Jt. Surg.* 60A: 905-910, 1978.
22. OHTA, Y., A. AR, AND L. E. FARHI. Solubility and partition coefficients for gases in rabbit brain and blood. *J. Appl. Physiol.* 46: 1169-1170, 1979.
23. OHTA, Y., AND L. E. FARHI. Cerebral gas exchange: perfusion and diffusion limitations. *J. Appl. Physiol.* 46: 1164-1168, 1979.
24. PHELPS, P., A. D. STEELE, AND D. J. MCCARTY. Significance of xenon-133 clearance from canine and human joints. *Arthritis Rheum.* 15: 360-370, 1972.
25. SHEPP, L. A., AND Y. VARDI. Maximum likelihood reconstruction for emission tomography. *IEEE Trans. Med. Imaging*, MI-1:113-122, 1982.
26. ST. ONGE, R. A., W. C. DICK, G. BELL, AND J. A. BOYLE. Radioactive xenon disappearance rates from the synovial cavity of the human knee joints in normal and arthritic subjects. *Ann. Rheum. Dis.* 27: 163-166, 1968.
27. SUSSKIND, H., H. L. ATKINS, S. H. COHN, K. J. ELLIS, AND P. RICHARDS. Whole body retention of radioxenon. *J. Nucl. Med.* 18: 462-471, 1977.
28. THOMAS, I. H., A. EVANS, AND D. N. WALDER. Saturation of mini-pig bone-marrow with nitrogen during exposure to compressed air. *Lancet* 127-129, 1982.
29. THOMAS, S. F., AND O. L. WILLIAMS. High-altitude joint-pains (bends): their roentgenographic aspects. *Radiology* 44: 259-261, 1945.
30. WEATHERSBY, P. K., AND L. D. HOMER. Solubility of inert gas in biological fluids and tissues: a review. *Undersea Biomed. Res.* 7: 227-296, 1980.
31. WEATHERSBY, P. K., K. G. MENDENHALL, E. E. P. BARNARD, L. D. HOMER, S. SURVANSI, AND F. VIERAS. The distribution of xenon gas exchange rates in dogs. *J. Appl. Physiol.* 50: 1325-1336, 1981.
32. WEATHERSBY, P. K., S. S. SURVANSI, AND P. MEYER. Spatial sensitivity of a planar positron camera. *Nucl. Instr. Methods Phys. Res.* 220: 571-574, 1984.
33. WEST, J. B. Studies in pulmonary and cardiac function using short-lived isotopes oxygen-15, nitrogen-13, and carbon-11. *Prog. At. Med.* 2: 39-64, 1968.
34. WOLF, J. Blood supply and nutrition of articular cartilage. *Folia Morphol.* 23: 197-208, 1975.
35. YOUNT, D. E. Skins of varying permeability: a stabilizing mechanism for gas cavitation nuclei. *J. Acoust. Soc. Am.* 65: 1429-1439, 1979.